PHILOSOPHICAL TRANSACTIONS OF THE ROYAL SOCIETY A

Phil. Trans. R. Soc. A (2012) **370**, 2557–2577
doi:10.1098/rsta.2011.0218

Water vapour foreign-continuum absorption in near-infrared windows from laboratory measurements

By Igor V. Ptashnik[1,3,*], Robert A. McPheat[2], Keith P. Shine[1], Kevin M. Smith[2] and R. Gary Williams[2]

[1]*Department of Meteorology, University of Reading, Earley Gate, PO Box 243, Reading RG6 6BB, UK*
[2]*RAL Space, Rutherford Appleton Laboratory, Didcot OX11 0QX, UK*
[3]*V.E. Zuev Institute of Atmospheric Optics, SB RAS, 1, Academician Zuev Square, Tomsk 634021, Russia*

For a long time, it has been believed that atmospheric absorption of radiation within wavelength regions of relatively high infrared transmittance (so-called 'windows') was dominated by the water vapour self-continuum, that is, spectrally smooth absorption caused by H_2O–H_2O pair interaction. Absorption due to the foreign continuum (i.e. caused mostly by H_2O–N_2 bimolecular absorption in the Earth's atmosphere) was considered to be negligible in the windows. We report new retrievals of the water vapour foreign continuum from high-resolution laboratory measurements at temperatures between 350 and 430 K in four near-infrared windows between 1.1 and 5 μm (9000–2000 cm^{-1}). Our results indicate that the foreign continuum in these windows has a very weak temperature dependence and is typically between one and two orders of magnitude stronger than that given in representations of the continuum currently used in many climate and weather prediction models. This indicates that absorption owing to the foreign continuum may be comparable to the self-continuum under atmospheric conditions in the investigated windows. The calculated global-average clear-sky atmospheric absorption of solar radiation is increased by approximately 0.46 $W m^{-2}$ (or 0.6% of the total clear-sky absorption) by using these new measurements when compared with calculations applying the widely used MTCKD (Mlawer–Tobin–Clough–Kneizys–Davies) foreign-continuum model.

Keywords: water vapour continuum; MTCKD continuum; atmospheric windows; collision-induced absorption; bimolecular complexes

1. Introduction

Water vapour is well established to be the dominant gas in determining the radiative balance of the Earth and its atmosphere [1]. Its infrared spectrum is characterized by strong absorption bands, made up of individual spectral lines resulting from rotational and vibrational–rotational transitions, interspersed

*Author for correspondence (piv@iao.ru).

One contribution of 17 to a Theo Murphy Meeting Issue 'Water in the gas phase'.

by regions of weaker absorption, known as 'windows'. In these windows, the absorption is dominated by the water vapour continuum, that is, by a slowly varying component of absorption that is also present, albeit with lesser (atmospheric) importance, in the absorption bands. The continuum is of importance both for the atmospheric radiative balance [2] and for remote sensing [3].

The nature and strength of the water vapour continuum absorption have been sources of uncertainty and controversy for many decades. Initially, focus was on the relatively strong continuum in the mid-infrared (8–12 μm; 1250–833 cm^{-1}) window, and early theories [4] attributed it to the accumulated absorption in the far (Lorentzian) wings of the spectral lines in the neighbouring absorption bands. Subsequent work (see especially [5]) established both the temperature and pressure dependence of the mid-infrared continuum, and importantly established that it possesses two components: a self-continuum, which is due to the interaction between water molecules, and a foreign continuum, which is due to the interaction of water molecules with other molecules, most notably nitrogen and oxygen in the Earth's atmosphere. The temperature dependence of the self-continuum lent support to the theory that the self-continuum could be due to water dimers. An alternative theory was that it was due to the far wings of distant spectral lines [6–8], which took into account that these lines must then depart from a Lorentzian profile far from the line centre to explain the observed continuum.

The debate on the cause of the continuum has not been resolved. However, in many atmospheric applications (in weather forecasting and climate prediction models, and in remote sensing applications), the debate has been sidestepped by the widespread adoption of a semi-empirical representation of the continuum. The Mlawer–Tobin–Clough–Kneizys–Davies (MTCKD) model [9,10] (see also http://rtweb.aer.com/continuum_frame.html), which superseded the Clough–Kneizys–Davies (CKD) model [7], represents the continuum by applying different line profiles which the authors of MTCKD attributed to two different physical mechanisms: collision-induced water monomer transitions dominate the in-band continuum, and far wings of spectral lines dominate in the windows. The CKD and MTCKD formulations represented an important advance, not least because they characterized the water vapour continuum throughout the infrared, rather than just in the mid-infrared window, and its importance in atmospheric radiative transfer was clearly demonstrated in Clough *et al.* [2].

However, because of its semi-empirical nature, most of the parameters for these line profiles in the MTCKD model do not have a direct physical meaning. Additionally, these parameters were derived by fitting the model continuum to available observations only in mid- and far-infrared (greater than 4 μm; less than 2600 cm^{-1}). These were then applied throughout the near-infrared and visible region, where there had hitherto been a paucity of suitable observations, because of the much weaker continuum at these wavelengths. Recent laboratory measurements in the near infrared (1–5 μm; 2000–10 000 cm^{-1}) [11,12]—supported in some spectral regions by earlier, less accurate, measurements—have established that the self-continuum within bands contains more spectral structure than given by the MTCKD model (which Ptashnik and colleagues [13,14] contend is strongly consistent with the dimer hypothesis). In the windows, the self-continuum absorption was found [15,16] to be typically an order of magnitude stronger than that given by MTCKD.

In contrast, the *foreign* continuum in the near infrared has received much less attention. In-band continuum measurements include those by Burch [17] (3500–4000 cm^{-1}) and Paynter *et al.* [12] (all four bands between 1300 and 7500 cm^{-1}). MTCKD is in broad agreement with these measurements, although, as with the self-continuum, the measurements indicate more spectral structure. The focus of this paper is on the retrieval of the *foreign* water vapour continuum in near-infrared windows.

Until recently, the contribution of the foreign-continuum absorption in the windows was considered to be negligible when compared with the self-continuum [7]. However, recent measurements in the 4 μm window by Baranov [18] clearly demonstrated that the foreign continuum can be up to two orders of magnitude stronger than in MTCKD model. We present here an experimental study of the foreign-continuum absorption in a broader spectral region, 2000–9000 cm^{-1}, in four near-infrared windows. The work can be considered as a companion paper to that of Ptashnik *et al.* [16], who derived the self-continuum of water vapour in the same wavelength region, using broadly the same measurement and analysis technique; indeed, as will be discussed, a consistent self-continuum is needed in order to separate the foreign continuum from the total (i.e. self plus foreign) continuum that is derived from the measurements. These measurements were performed within the UK-based Continuum Absorption at Visible and Infrared wavelengths and its Atmospheric Relevance (CAVIAR) consortium, and hence the new continuum is often referred to in this work as the CAVIAR continuum. The measurement techniques are described in §2, the analysis method is described in §3 and results are presented in §4. The implication of these new measurements for understanding the cause of the foreign continuum in near-infrared windows is briefly discussed in §5. The impact of the new data on atmospheric absorption of solar radiation is considered in §6.

2. Experimental technique

The measurement technique closely follows that described in detail by Ptashnik *et al.* [16]. Briefly, spectra were recorded using a Bruker IFS-125 high-resolution Fourier transform spectrometer (FTS) at the Rutherford Appleton Laboratory (RAL) Molecular Spectroscopy Facility (http://www.msf.rl.ac.uk) using a multi-pass short-path absorption cell (SPAC), based on the White [19] arrangement. This has a total optical path length of 17.7 m, and allowed highly stable measurements to be conducted at total pressures of up to about 5 atm and temperatures from 350 to 430 K (table 1). (Lower temperature measurements would have been desirable, for atmospheric applications, but the signal-to-noise ratio would have been inadequate. In any case, as will be discussed in §4, the foreign continuum, unlike the self-continuum, has only a weak temperature dependence.) Measurements were performed at a spectral resolution of 0.1 cm^{-1}, high enough to resolve individual spectral lines. The impact of instrumental lineshape function was found to be negligible on the retrieved continuum. The cell and the transfer optics were housed in evacuated chambers (typically at pressures of less than 10^{-4} mbar) to remove absorption from laboratory air and to provide thermal insulation. Saturation vapour pressures for each measurement temperature are shown in table 1. The relative humidity

Table 1. Experimental conditions: temperature T, approximate water vapour P_{H_2O} and air P_{air} pressures and path length. The saturated pressure for each temperature is shown in the first column for reference. The spectral resolution and number of FTS scans were chosen to ensure that single spectral lines are spectrally resolved and the signal-to-noise ratio (r.m.s.) was on average not less than 700. The superscript against each pressure denotes the number of measurements made at this pressure when it was more than one.

saturated H_2O pressure (mbar)	T (K)	$P_{H_2O} + P_{air}$ (mbar)	path length (m)
416	350	$266 + 4700$	17.7
970	372	$500 + 4500$	
2500	402	$600 + 4400^{(2)}$	
5700	431	$600 + 4400^{(2)}$	
resolution (cm^{-1})		0.1	
no. scans		500–1000	

Table 2. Details of the RAL MSF spectrometer and gas cell configuration used in this work.

spectral range	2000–10 000 cm^{-1}
source	50 W quartz tungsten halogen bulb
detector	indium antimonide
beam splitter	calcium fluoride
optical filter	none
apodization	boxcar
cell window materials	sapphire (inner)/CaF_2 (outer)
SPAC mirror coatings	gold
pressure gauge	Setra Barocel Model 725, modified to operate temperature controlled to 473 K using thin film heaters, and Cal Controls 9300 temperature controller ± 0.15% accuracy
humidity sensors	Sensirion SHT75, ±1.8% relative humidity accuracy
thermometry	platinum resistance thermometers at seven positions, Labfacility IEC 751 class A, cell temperature stability ±0.2 K

in the cell was at most 75 per cent and was normally much less than this to ensure that there was no condensation on the cell optics. Table 2 provides the details of the spectrometer and gas cell configurations used here.

The measurements at each pressure and temperature used the following procedure: (1) background measurement with an empty cell; (2) background measurement with approximately 5000 mbar of artificial air (Air Products Zero Air, 79.1% N_2 and 20.9% O_2); (3) sample measurements of a mixture of H_2O vapour (VWR AnalaR Normapur) with air, so that the total pressure was the same as step 2; (4) same as step 2; (5) same as step 1. The sample measurements (step 3) were typically made in a mixture of 300–600 mbar water vapour, depending on temperature, and 4400–4700 mbar of air (table 1). The background measurements with an empty cell and with air were carried out, first, to ensure that any possible cell distortion due to pressure was taken into account and,

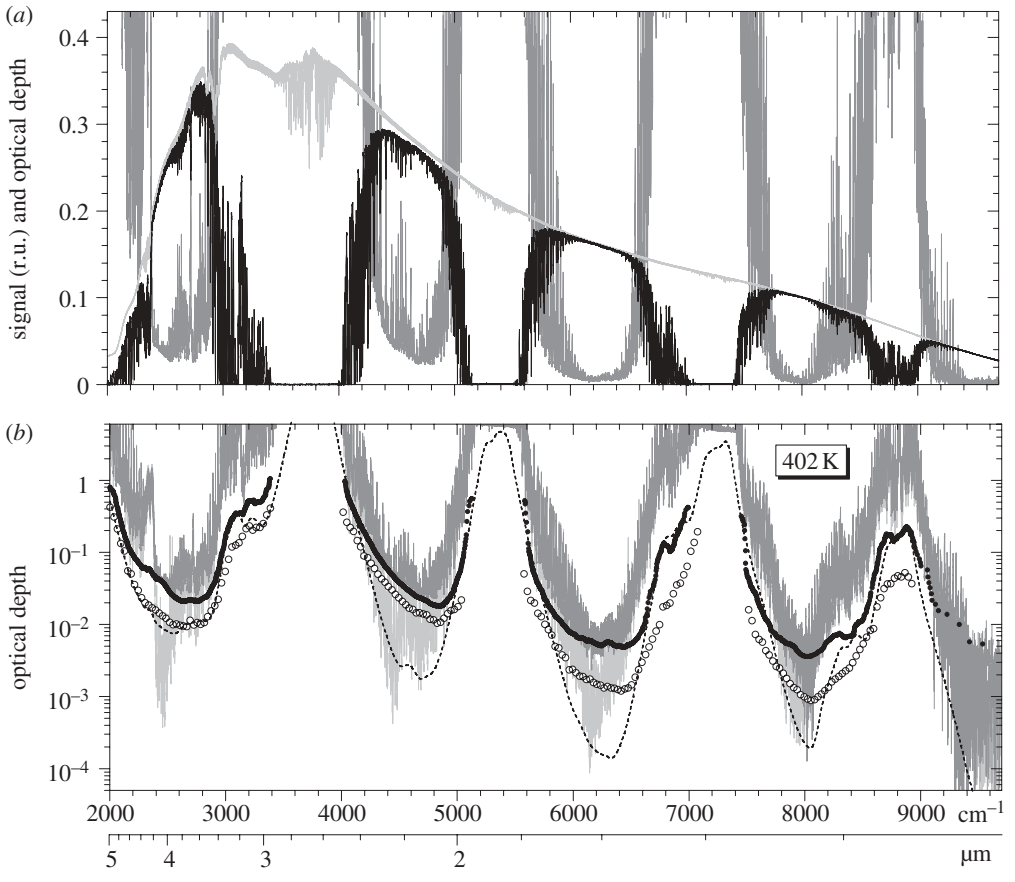

Figure 1. (*a*) An example of the FTS signals (relative units) for background (light grey lines) and sample (black lines) measurements, and the derived water vapour optical depth (dark grey lines) as a function of wavelength and wavenumber. Temperature, 402 K; water vapour pressure, 600 mbar; air pressure, 4400 mbar; total path length, 17.7 m. (*b*) Simulated spectrum (UCL08 line list [20], light grey lines) calculated up to 25 cm^{-1} from the line centres without a plinth; experimental RAL (dark grey lines) spectrum; MTCKD-2.5 (dashed lines) total continuum [9,10]; optical depth of the total (i.e. self plus foreign) continuum (dots) derived as a spectrally smoothed difference between RAL and UCL08 in microwindows between lines; contribution from the self-continuum (circles) derived using data [16] for the same temperature.

second, to separate the contribution from pure O_2 and N_2 absorption from the water vapour foreign continuum. The final background was usually derived as an average between steps 2 and 4. There was no noticeable impact of pressure distortion of the cell. Figure 1*a* shows an example of the background, sample and retrieved optical depth spectra. The good baseline stability can also be seen from the very small difference between the background and sample spectra in the window 9600 cm^{-1}, in which absorption was negligible for the measurement conditions used here.

The water sample was purified by two cycles of freezing, evacuating with a turbo pump and thawing to remove atmospheric contaminants. Empty-cell background measurements were performed when the measured cell pressure was

less than 2×10^{-3} mbar. During background measurements, there was a trace amount of water vapour in the cell even after evacuation (figure 1*a*) owing to water molecules that had been adsorbed on the inner surfaces of the cell during sample measurements. The spectroscopic absorption is noticeable near the centre of the water vapour bands at wavelengths not used here in the derivation of the continuum.

The strong signature of a CO_2 band was usually visible in the sample spectra in the region near 2300 cm^{-1}, which was caused by very small amounts of CO_2 (*ca* 3–5 ppmv) dissolved in the liquid water sample. This signature could not always be completely removed by subtracting a simulated CO_2 spectrum, and this sometimes affected the retrieved continuum in the spectral region 2270–2370 cm^{-1}.

3. Data processing

(*a*) *Continuum retrieval*

Again, the retrieval technique closely follows that described in Ptashnik *et al.* [16]. The optical depth τ_m of the measured spectra is given by

$$\tau_{\mathrm{m}}(\nu) = -\ln\left\{\frac{I(\nu)}{I_{\mathrm{o}}(\nu)}\right\}, \tag{3.1}$$

where I is the measured intensity of a sample measurement, I_{o} is the intensity of a background measurement and ν is the wavenumber in cm^{-1}. The optical depth of the total (foreign plus self) continuum τ_{c} in each microwindow was then derived following a procedure similar to CKD [7], so that

$$\tau_{\mathrm{c}}(\nu) = \tau_{\mathrm{m}}(\nu) - \Sigma\tau_{\mathrm{line},i}(\nu - \nu_i), \tag{3.2}$$

where $\tau_{\mathrm{line},i}(\nu - \nu_i)$ is the local Lorentzian[1] contribution from ith H_2O spectral line, centred at ν_i within 25 cm^{-1} of the microwindow. In the CKD approach, the Lorentzian contribution of monomer lines is calculated without the 25 cm^{-1} 'CKD plinth' (figure 2); we follow the same approach to enable a direct comparison with the MTCKD continuum model. Hence, a part of the continuum derived here belongs to spectral line absorption. This component is very small for the work reported here, contributing less than 1 per cent in the middle of the windows [16].

The contribution from the spectral lines was calculated using a line-by-line code [21] and the UCL08 (University College London, UK) compilation of H_2O line parameters [20], which contains a number of weak water vapour lines not catalogued in the HITRAN-2008 [22] spectral line database. Accounting for these weak lines markedly impacts on the self-continuum retrieval in the 6300 and 8000 cm^{-1} windows [16].

Because the baseline in this work was derived from background measurements at 5000 mbar air pressure (in our case a mixture of N_2 and O_2), the contribution from N_2–N_2 (near 2400 cm^{-1}) and O_2–O_2 (near 6400 and 7900 cm^{-1})

[1]At the wavenumbers of interest here, the Lorentzian line shape is equivalent, to high accuracy, to the Van Vleck and Huber lineshape used by Clough *et al.* [7].

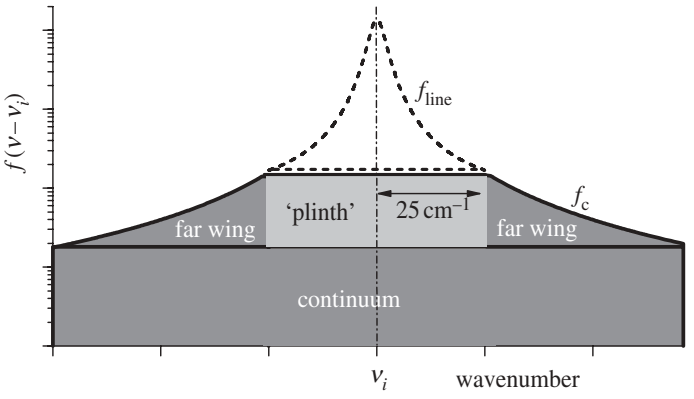

Figure 2. Dashed and solid curves schematically outline, respectively, the local (f_{line}) and far-wing continuum contribution (f_c) from every spectral line to the total absorption, according to the definition in the CKD model [7]. The grey area shows the total continuum absorption, which, in the CKD/MTCKD definition, includes the 25 cm^{-1} 'plinth' (light grey) from under every line ('plinth' + f_{line} = Lorentzian). Thus, in order to make the continuum smoother and more amenable to tabulation in the CKD/MTCKD approach, only the f_{line} part of every spectral line is subtracted from the experimental spectrum to derive the continuum, leaving the weak Lorentzian plinth as part of the continuum. The contribution of this plinth to the total continuum does not exceed 5–7% within bands and 1% in windows for the conditions investigated here.

collision-induced absorption (CIA) bands was naturally present in the baseline measurement, and thus was automatically excluded from the measured continuum τ_{m} via the use of equation (3.1). A small correction was then applied to account for the difference in the CIA contribution between 5000 mbar (background measurement) and 4400–4700 mbar (air pressure at sample measurements).[2] However, the small bumps still remaining in the retrieved continuum near 6300–6400 and 7800–7900 cm^{-1} (figure 1*b*) can be attributed to imperfect subtraction of O_2 CIA.

The impact of uncertainty in water line parameters on the retrieved continuum is usually small in the windows. Nevertheless, in order to diminish this impact as much as possible, the total continuum data derived from equation (3.2) (light grey points in figure 3) were filtered to exclude points close to the line centres, where the impact of any errors in line parameters is maximum. An example of the resulting total continuum is shown in figure 3 by the solid squares.

To derive optical depth of the foreign continuum τ_{f}, the self-continuum optical depth τ_{s}, retrieved from pure water vapour measurements by Ptashnik *et al.* [16], was subtracted from the total continuum: $\tau_{\text{f}} = \tau_{\text{c}} - \tau_{\text{s}}$. Figure 1*b* shows an example of the total continuum retrieved at 402 K in a mixture of 600 mbar H_2O with 4400 mbar air, and the contribution from the self-continuum for these conditions. All stages of the retrieval are shown in a particular spectral region in figure 3.

[2]An extra part of the CIA absorption, implicitly subtracted when deriving τ_m from equation (3.1), and equal to $\tau_{\text{air}}(5000\,\text{mbar}) \times [1 - P_{\text{air}}(\text{sample})^2/5000^2]$, was added back to the total continuum τ_{c}. The τ_{air} was derived by comparing empty cell and air-filled background measurements.

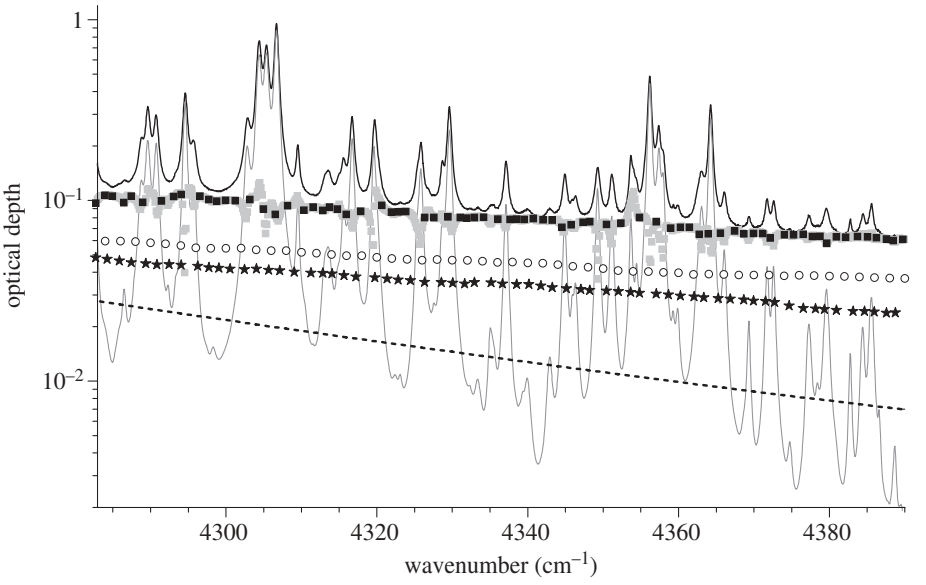

Figure 3. An example of the consecutive stages of the foreign-continuum retrieval (stars) in a small spectral interval: (i) the total continuum (black squares) is derived as a spectrally smoothed and filtered difference (grey squares) between the experimental RAL (solid black line) spectrum and the line-by-line simulation using UCL08 (grey line) data [20] in the microwindows between lines; (ii) the foreign continuum is derived as a spectrally smoothed difference between the total and self-continuum (circles) [16]. The total MTCKD-2.5 continuum (dashed line) [9,10] is shown for comparison. The data correspond to: $T = 402\,\mathrm{K}$, $P_{H_2O} = 600\,\mathrm{mbar}$, $P_{air} = 4400\,\mathrm{mbar}$, $L = 17.7\,\mathrm{m}$.

The cross section (cm^2 $molecule^{-1}$ atm^{-1}) of the foreign continuum was then derived as

$$C_f(\nu, T) = \frac{\tau_f(\nu)}{\rho_s P_f L} \equiv \tau_f(\nu)\frac{kT}{P_s P_f L}, \tag{3.3}$$

where ρ_s and P_s are water vapour gas number density and partial pressure, respectively; P_f is the air pressure in the sample measurement, k is the Boltzmann constant, T is the temperature and L is the absorbing optical path length. Finally, a factor $T/296$ is applied to all data to convert them to the CKD/MTCKD definition [7,9], in which the cross section at each temperature is normalized to the number density at 1 atm, 296 K. Thus, in the MTCKD definition, the temperature dependence of number density is excluded from the continuum cross section.

(*b*) *Error of the derived continuum*

In the relatively transparent windows, the contribution from local lines in the microwindows between these lines is usually negligible when compared with the continuum absorption (see the 'UCL08 lines' curve in figure 3). Thus, in window regions, the main source of experimental error for the continuum retrieval is *baseline uncertainty*. That is why, as described in §2, additional measurements were taken to ensure good baseline stability.

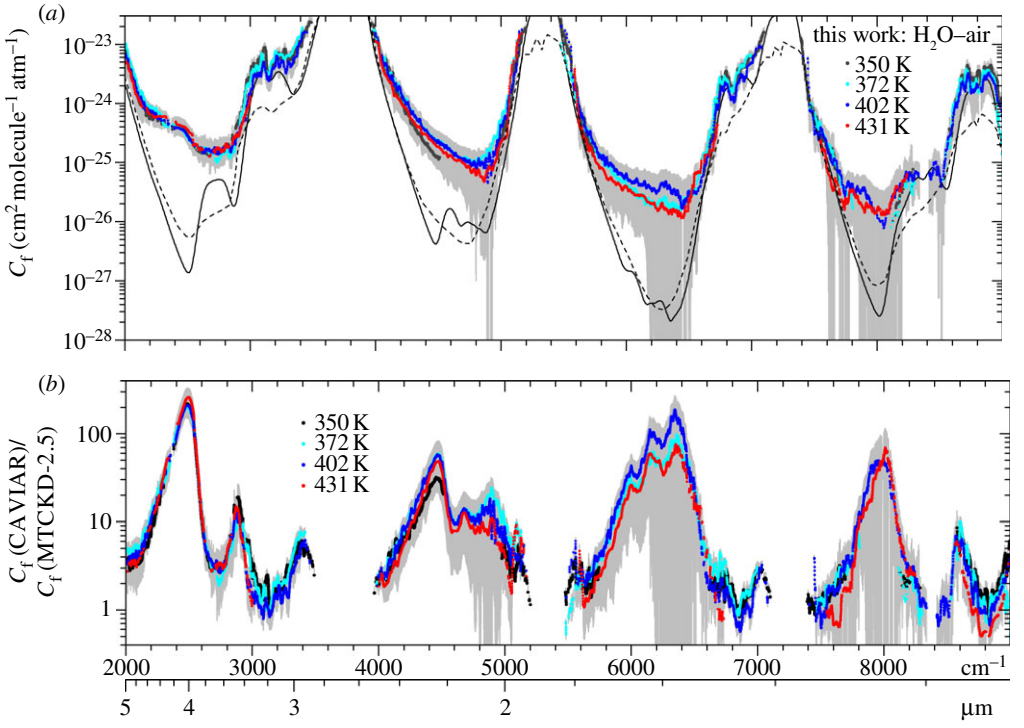

Figure 4. (*a*) Water vapour foreign (H_2O–air) continuum cross sections derived in this work at 350, 372, 402 and 431 K are shown by different colours. The MTCKD-2.5 (solid line) [9,10] water vapour foreign continuum (temperature independent) and the Tipping & Ma [8] H_2O-N_2 far-wing model (296 K, dashed line) are shown for comparison. (*b*) Ratios of the (CAVIAR) foreign continuum derived here to those in the MTCKD-2.5 model at different temperatures. The shaded areas show the estimated total error of the derived continuum. (Online version in colour.)

The total uncertainty in the foreign continuum retrieved in this work and presented in figure 4*a* and table 3 originates mainly from two sources: experimental error of the total continuum and error in the self-continuum derived in Ptashnik *et al.* [16]. Experimental error of the continuum retrieval in the windows is dominated by instability in the baseline. This was estimated as half of the difference between the average background spectra before and after every sample measurement. This generally did not exceed on average 0.4 per cent of the value of the FTS signal in the windows, leading to an uncertainty in optical depth varying typically from 0.002 to 0.004 in the spectral region under investigation. The relative error in the self-continuum derived in Ptashnik *et al.* [16] does not exceed 20–30% in these windows for temperatures between 374 and 430 K, leading on average to a similar or smaller relative error in the derived foreign continuum. In the 1.6 and 1.2 μm windows, the errors above 30 per cent in the derived foreign continuum were caused by uncertainty in the baseline rather than by error in the self-continuum.

On the edges of the windows, i.e. closer to the water vapour bands, the error in the derived continuum becomes more dominated by uncertainty in the parameters of the spectral lines, whose close wings must be subtracted to retrieve

Table 3. Spectrally smoothed absorption cross section $C_f(\nu)$ (10^{-25} cm^2 molecule^{-1} atm^{-1}) of the foreign continuum, derived in this work at 400 K. The total error of the retrieval is presented by ΔC_f. Cross sections are given using the CKD [7] definition.

ν (cm^{-1})	C_f	ΔC_f	ν (cm^{-1})	C_f	ΔC_f	ν (cm^{-1})	C_f	ΔC_f
2010	62	17	4470	2.4	1.3	6720	8.8	1.7
2040	36	12	4500	2.1	1.2	6750	13	2.4
2070	22	8	4530	2	1.1	6780	18	2.4
2100	14	5.2	4560	1.8	1	6810	17	3
2130	9.1	3.8	4590	1.6	0.9	6840	13	2.5
2160	6.9	2.7	4620	1.4	0.9	6870	16	3.2
2190	6.4	2.4	4650	1.2	0.9	6900	23	3.7
2220	5.8	2.2	4680	1.1	0.8	6930	30	5.2
2250	5.5	2	4710	1	0.8	6960	42	6.5
2280	5	1.7	4740	0.95	0.8	6990	51	8
2310	4.8	1.6	4770	0.89	0.8	7020	61	9.6
2340	4.7	1.5	4800	0.86	0.8	7440	40	4.7
2370	4.6	1.4	4830	0.92	0.7	7470	13	1.6
2400	4.3	1.3	4860	0.88	0.7	7500	4.7	1.4
2430	3.7	1.3	4890	0.9	0.9	7530	3.3	1.1
2460	3.5	1.2	4920	1	0.9	7560	2.9	0.8
2490	3	0.9	4950	1.5	0.9	7590	2.2	0.6
2520	2.4	0.8	4980	2.5	1.1	7620	1.5	0.6
2550	2	0.8	5010	4.4	1.4	7650	0.97	0.5
2580	1.8	0.7	5040	7.4	1.7	7680	0.79	0.4
2610	1.6	0.6	5070	16	2.9	7710	0.5	0.32
2640	1.5	0.6	5100	27	6	7740	0.41	0.32
2670	1.6	0.7	5130	46	7.5	7770	0.32	0.32
2700	1.5	0.7	5550	54	9.7	7800	0.3	0.31
2730	1.5	0.6	5580	23	9.3	7830	0.27	0.27
2760	1.5	0.6	5610	15	3.1	7860	0.27	0.27
2790	1.6	0.7	5640	7.6	1.7	7890	0.26	0.27
2820	1.8	0.7	5670	4.4	1.2	7920	—	—
2850	1.7	0.7	5700	2.8	1	7950	—	—
2880	2.3	0.9	5730	2.1	0.9	7980	—	—
2910	3.4	1.1	5760	1.5	0.7	8010	—	—
2940	6.2	1.7	5790	1.1	0.6	8040	—	—
2970	9	2.7	5820	0.94	0.53	8070	—	—
3000	17	3.6	5850	0.8	0.48	8100	—	—
3030	24	5.3	5880	0.72	0.45	8130	—	—
3060	30	6.9	5910	0.6	0.41	8160	—	—
3090	35	10	5940	0.52	0.39	8190	0.36	0.33
3120	34	11	5970	0.47	0.35	8220	0.44	0.37
3150	27	7.5	6000	0.45	0.35	8250	0.51	0.42
3180	37	10	6030	0.38	0.34	8280	0.53	0.38
3210	48	12	6060	0.37	0.33	8310	0.52	0.43
3240	51	12	6090	0.36	0.33	8340	0.38	0.38
3270	46	12	6120	0.32	0.29	8370	0.35	0.41
3300	44	13	6150	0.32	0.28	8400	0.34	0.42
3330	49	14	6180	0.29	0.28	8430	0.55	0.45
3360	69	21	6210	0.26	0.28	8460	0.71	0.65

(*Continued.*)

Table 3. (*Continued.*)

ν, cm^{-1}	C_f	ΔC_f	ν, cm^{-1}	C_f	ΔC_f	ν, cm^{-1}	C_f	ΔC_f
3390	100	23	6240	—	—	8490	0.65	0.65
4020	95	21	6270	—	—	8520	0.98	0.9
4050	62	14	6300	—	—	8550	1.7	0.65
4080	43	11	6330	—	—	8580	3.2	1.3
4110	32	8.6	6360	—	—	8610	6	1.6
4140	24	6.5	6390	—	—	8640	11	2.1
4170	19	5.2	6420	—	—	8670	16	3
4200	16	4.3	6450	—	—	8700	22	3.7
4230	11	3.5	6480	—	—	8730	22	4.2
4260	9.2	3	6510	—	—	8760	17	3.2
4290	7	2.5	6540	0.27	0.33	8790	18	3.2
4320	5.8	2.2	6570	0.37	0.35	8820	20	4.2
4350	4.8	1.9	6600	0.59	0.4	8850	23	4.6
4380	3.7	1.7	6630	1.1	0.6	8880	28	5.6
4410	3.2	1.6	6660	2.7	0.7	8910	25	5
4440	2.7	1.4	6690	3.9	0.9	8940	18	3.6

the continuum. According to our estimations, this uncertainty on average may lead to 10–15% error in the retrieved continuum closer to the band centres at the investigated temperatures. The contribution to experimental errors caused by uncertainties in measured water vapour pressure and temperature in the cell (table 2) usually did not exceed 5 per cent and were less important than the baseline error.

4. Results

Figure 4 shows the cross sections of the foreign (H_2O–air) continuum C_f, derived in this work at four temperatures, and the ratio of these cross sections to those in the MTCKD model. As was stressed earlier, the contribution from the water vapour self-continuum (H_2O-H_2O) and from N_2-N_2 and O_2-O_2 CIA was excluded from C_f. The MTCKD-2.5 model [9,10] and the far-wings model of Tipping & Ma [8] are presented for comparison.

Figure 5 shows in more detail the 4 µm (2500 cm^{-1}) window. The spectrally smoothed foreign continuum retrieved at 402 K is compared with the recent experimental data of Baranov [18] for H_2O-N_2 continuum absorption. In this window, our data are on average in good agreement with those of Baranov [18], despite the fact that Baranov [18] derived the foreign continuum in the mixture H_2O-N_2, while in our work it was derived in H_2O–air. Similar to the results in Baranov [18], our data demonstrate foreign-continuum absorption up to a factor of 200 stronger than MTCKD-2.5 in this window (figure 4*b*). Although, in the 2000–2200 cm^{-1} region and near 2900 cm^{-1}, our data are about a factor of 1.5 higher than those reported in Baranov [18], the differences mostly lie within the total uncertainty of both retrievals. On average, results from Baranov [18]

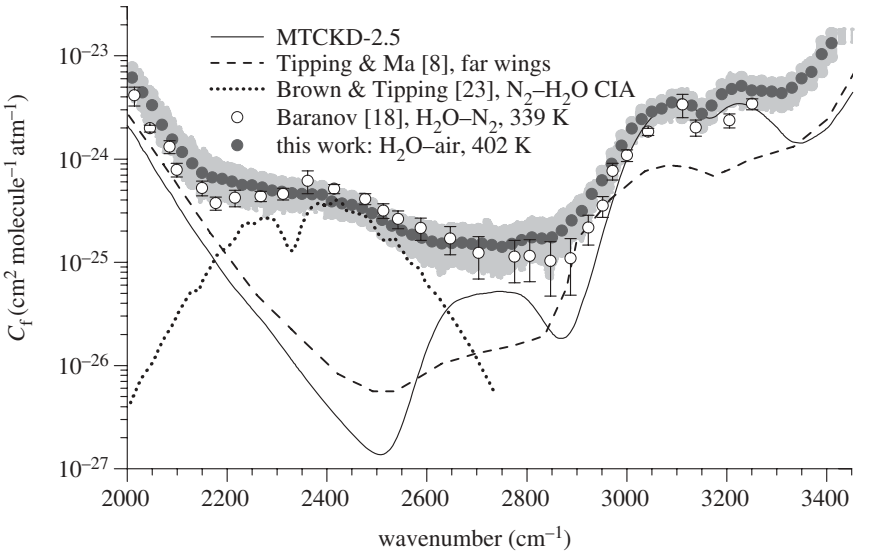

Figure 5. Smoothed values of the water vapour foreign (H_2O–air) experimental cross sections derived in this work at 402 K in the 4 µm window are shown together with the MTCKD-2.5 [9,10] foreign-continuum model (temperature independent), the Tipping & Ma [8] H_2O-N_2 far-wing model (296 K), the Brown & Tipping [23] *ab initio* prediction for N_2-H_2O CIA and the Baranov [18] experimental data for the foreign (H_2O-N_2) continuum at 339 K. The shaded area shows the estimated total error of the continuum retrieval in this work.

show less uncertainty than our data in this window, which is perhaps caused by a 2–3 times larger $L \times P_s$ parameter in Baranov [18] than in our experiments. At the same time, the error bars [18] at the edges of the window (i.e. near 2000 and above 3000 cm^{-1}) seem too optimistic (less than 5%), and obviously do not include systematic errors that may be caused by uncertainties in line parameters.

It is clear from figure 4 that in three other near-infrared windows, where the foreign continuum is investigated for the first time to our knowledge, the situation is quite similar to the 4 µm window. Although the uncertainty in the foreign continuum retrieved in the centre of the 1.6 µm window, and especially in the 1.2 µm window, reaches 100 per cent (the optical depth is comparable to or less than the baseline error), the strength of the continuum absorption in the less uncertain regions within these windows is considerably larger than that in the MTCKD model.

Thus, our results reveal that, in a way similar to the self-continuum absorption [15,16], the foreign H_2O–air continuum within four investigated near-infrared windows is typically of one to two orders of magnitude stronger than that in the MTCKD model (figure 4*b*). As noted earlier, unlike the present work, the MTCKD foreign continuum in these spectral regions was not based on measurements, but is rather a result of the application of model parameters derived at longer wavelengths. Specifically, these parameters are introduced within the MTCKD approach to construct semi-empirical H_2O line profiles

including the far wings; they are derived by fitting the model to an experimental mid- and far-infrared continuum and then are applied to predict the continuum at shorter wavelengths.

In the MTCKD model, the cross section of the water vapour foreign continuum is assumed to be temperature independent. The measurements here support that assumption. Figure 4 shows that, if there is any temperature dependence of the experimental foreign-continuum cross section, it is rather weak in the investigated temperature range, and lies within the uncertainty of our current retrieval. Only in some spectral regions closer to the band centres is there an indication of a weak negative temperature dependence of the foreign continuum.

The smoothed data of the foreign continuum retrieved in this work at 400 K are tabulated in table 3, with a sampling step of 30 cm^{-1}.

5. Discussion

Although the prime purpose of this paper was to present the new measurements, we briefly discuss the implications of these new measurements for understanding the causes of the foreign continuum. The calculation of the far-wing absorption of strong water monomer lines in the theoretical approach by Tipping & Ma [8] (figure 4*a*) is an order of magnitude smaller than the continuum retrieved here. So, one can assume that either the far-wing absorption by water monomers cannot contribute markedly to the derived continuum in these windows and at the temperatures under discussion or the current theory is significantly in error.

Similarly, we do not believe that local lines can contribute significantly to the derived continuum. The Lorentzian contribution from local lines (within 25 cm^{-1}) has been subtracted in this work in order to derive the continuum (figure 3). The Lorentzian line profile is reasonably good (on average within 5–10%) for the simulation of the spectral line contribution within approximately 5 cm^{-1} of the line centre and up to 5 atm pressure [24]. In the windows investigated here, the contribution from local lines, situated further than 5–10 cm^{-1} from each microwindow, was usually very small.

Finally, the possible contribution from water monomer line mixing to the retrieved continuum is expected to be rather weak in most microwindows at pressures below 5 atm [24]. In any case, for the measurement conditions used here, line mixing is likely to be detectable only for particular and quite rare pairs of water vapour lines, satisfying certain selection rules [25], and hence is unlikely to have the continuum-like nature derived here.

Taking these points into account, we suggest that the foreign continuum derived here can only be explained in terms of bimolecular absorption (BA), which is proportional to the product of the water vapour and nitrogen (or oxygen) partial pressures. Indeed, it was shown by Brown & Tipping [23] that the nitrogen fundamental absorption band, when induced by collisions between N_2 and H_2O molecules, is much stronger than that in pure nitrogen. This enhancement is not accounted for in the MTCKD model of the 'foreign' N_2–H_2O continuum. Here we put N_2 in first place to underline that it is CIA from the fundamental nitrogen band (or the 'N_2-foreign' continuum), rather than collision-modified absorption due to transitions in the water molecule (or

the 'H_2O-foreign' continuum). The result of calculations [23] of CIA[3] of the fundamental N_2 band, arising from interaction between N_2 and H_2O molecules, is presented in figure 5, and shows a reasonable agreement with our retrieval at around 2400 cm^{-1}. *Ab initio* calculations of the N_2-H_2O CIA band intensities at different temperatures [27], performed using a more sophisticated potential energy surface and dipole surface for the N_2-H_2O complex, has shown good agreement with experimental evaluations made in Baranov *et al.* [27] on the basis of measurements [18].

Thus, there is direct evidence that, in the 2200–2500 cm^{-1} spectral region, the continuum under atmospheric conditions should be strongly affected by N_2-H_2O CIA absorption. It was suggested in Baranov *et al.* [27] that overtones of the nitrogen fundamental band perturbed by water may also cause more pronounced intensity of the N_2-H_2O foreign continuum at higher wavenumbers. The latter, however, according to our results, would require the CIA intensity of the first overtone for the N_2-H_2O system to be rather strong; it would have to be weaker than the fundamental N_2-H_2O CIA band by not much more than a factor of 5–6 (the ratio of the foreign continuum derived here in the 2300–2400 and 4600–4800 cm^{-1} spectral regions). Besides, if this overtone contributed significantly to the continuum, it would have appeared as a broad spectral feature centred near 4800 cm^{-1}, which does not seem to be the case in the experimentally derived continuum (figure 4*a*). Hence, the origin of this continuum, which is much stronger than predicted by the MTCKD H_2O-foreign and/or N_2-foreign continuum in the windows above 2200–2500 cm^{-1}, is unclear. It is possible also that it results from H_2O-N_2, H_2O-O_2 and other complexes [28–30]. However, this issue requires further investigation. In addition to the uncertainty in intensities, the spectral width and shape of the absorption due to these complexes is poorly known, which particularly strongly influences the amount of absorption within the windows. Thorough statistical division of molecular pair states in phase space [29,31] and classic trajectory analysis [32] seem to be promising tools to help answer the question about the fraction of bound, quasi-bound and free-pair states that can be involved in BA at close to atmospheric conditions.

The negligible (within the accuracy of these experiments) temperature dependence of the detected 'foreign' continuum compared with the strong temperature dependence of the H_2O self-continuum [16] does not contradict the idea of absorption by H_2O-X complexes. The much smaller dissociation energy of the H_2O-N_2 complex compared with H_2O-H_2O (350 and 1700 K, respectively [28]) will cause a much weaker temperature dependence of the equilibrium constant than is the case for H_2O-H_2O. For example, the analytical estimation given in Vigasin [28] (see also [33]) would show only an approximately 20–30% change in the expected absorption by such complexes in the temperature range 370–430 K investigated here. Moreover, for such small dissociation energies,

[3]Strictly speaking, the term 'CIA', by its origin, should be used only for BA arising mostly from transitions not involving long-lived quasi-bound and true-bound states [26]. Hence, until an exact partitioning of pair states is performed, using a general term 'bimolecular absorption' could be more advisable [14]. At the same time, traditionally the term 'CIA' is often used with respect to BA spectra in the region of the dipole-forbidden transition in the highly symmetrical parent monomers (such as N_2 in the discussion above). In that case, it is important to realize that there may be a possible contribution from bound and quasi-bound complexes to this 'CIA'.

most of the contribution at room temperature can be expected to originate from quasi-bound rather than bound complexes [14,29], which may cause an even weaker temperature dependence owing to effective averaging of the intermolecular potential by nearly free rotation of the monomers in such complexes. For the 2.1, 1.6 and 1.2 µm windows, such a relatively small temperature-related change would lie within the average uncertainty of the continuum retrieval in this work, and so cannot be clearly detected; the N_2-H_2O CIA in the 4 µm window, according to Baranov *et al.* [27], is expected to have an even weaker temperature dependence within the temperature range investigated here.

6. Implication for near-infrared absorption by the atmosphere

Until recently, the contribution of the foreign continuum to the absorption within windows was considered to be negligible when compared with the self-continuum [7]. However, the much stronger foreign continuum derived here in four near-infrared windows may markedly change this perception. Figure 6 shows the simulated vertical optical depth (0–100 km; mid-latitude summer atmosphere; column water vapour amount of 2.7 g cm^{-2}) caused by the MTCKD-2.5 continuum (total self and foreign). Continuum absorption by CO_2, N_2, O_2 and O_3 is also included in the calculation. Figure 6 shows also the optical depth using MTCKD-2.5 but with the water vapour self-continuum modified according to the CAVIAR data [16], and MTCKD with both self- and foreign-continuum coefficients modified using CAVIAR data. Taking into account the very weak temperature dependence of the foreign continuum found in Baranov [18] and in this work, we used the same cross section as presented in table 3 for 400 K for our calculations. According to the new data, the contribution of the foreign continuum to the total self- plus foreign-continuum vertical optical depth in the investigated windows may be quite significant, reaching 50 per cent in some spectral intervals.

We have also estimated the impact of the newly derived water vapour foreign continuum on the calculated clear-sky absorption of solar radiation in near-infrared windows. The line-by-line code [21] was used for high (0.001 cm^{-1}) spectral resolution calculations of optical depth for 18 atmospheric layers of clear-sky mid-season zonal-mean atmospheric profiles [34] at a latitudinal resolution of 10°. In addition to water vapour, the atmospheric profiles also include CO_2, O_3, CH_4, O_2 and N_2. We used H_2O line parameters from the UCL08 line list [20], and the HITRAN-2008 database [22] for all other gases. Irradiance calculations were performed using these optical depth spectra as input to the Discrete Ordinate (DISORT) code of Stamnes *et al.* [35], with the four-stream approximation to account for Rayleigh scattering. The calculations use the top-of-the-atmosphere solar irradiance compiled by Fontenla *et al.* [36], which represents the solar spectrum at a spectral resolution of 0.1 cm^{-1}.

Figure 7*a* displays the calculated spectrum of the total solar flux at the surface, and the extra absorption caused by the difference between the MTCKD-2.5 and its modified versions with either water vapour self-continuum or foreign continuum within the windows replaced by CAVIAR data. The calculation was performed for a typical tropical atmosphere, overhead sun and a column water vapour amount of 4.7 g cm^{-2}. The cumulative extra absorption in the whole 2000–10 000 cm^{-1} spectral region owing to the 'CAVIAR enhancement' to the

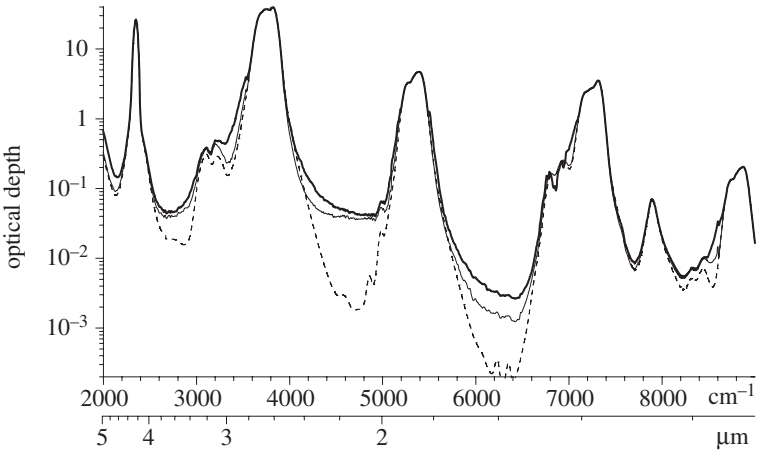

Figure 6. Simulated optical depth of the vertical atmospheric layer (0–100 km; mid-latitude summer; column water vapour amount of 2.7 g cm^{-2}) caused by the MTCKD-2.5 [9] continuum model (dashed line) including H_2O (self and foreign), CO_2, N_2, O_2 and O_3 continua. The thin and thick solid lines show, respectively, the MTCKD-2.5 with the water vapour self-continuum modified in the windows according to the CAVIAR data [16], and the MTCKD-2.5 modified in the windows according to the CAVIAR data for both the self- and foreign (this work) continuum.

H_2O self-continuum in the windows [16] is 3.3 W m^{-2}, while the CAVIAR foreign continuum contributes a further 1.8 W m^{-2} when compared with the MTCKD-2.5 model. Although the total water vapour continuum absorption in the atmosphere has approximately the same strength in the 2.1 and 4 μm windows (figure 6), the additional absorption originates primarily from the 2.1 μm (4000–5000 cm^{-1}) region because the extraterrestrial solar flux in this region is stronger (by about a factor of 3) than in the 4 μm window.

It is interesting that the absorption in the investigated spectral region, caused by the MTCKD-2.5 water vapour self- and foreign continuum itself, when compared with the calculation including only local (within 25 cm^{-1}) spectral lines contribution, is 3.2 and 1.85 W m^{-2}, respectively, for the tropical atmospheric model.[4] Thus, the CAVIAR corrections actually double the near-infrared absorption owing to the water vapour continuum when compared with the MTCKD-2.5 model, making it equal to about 6.5 and 3.7 W m^{-2} for the self- and foreign part, respectively.

Table 4 compares these values with the results presented by Kjaergaard *et al.* [30], who used band intensities and positions derived from *ab initio* quantum chemical calculations to estimate possible absorption due to a range of water vapour complexes. The extra absorption due to the modified foreign continuum, estimated here as 3.7 W m^{-2} for the tropical clear-sky atmosphere and overhead sun, is somewhat larger than the result of calculations [30]—2.3 W m^{-2} for H_2O–N_2 and H_2O–O_2 complexes assuming a Lorentzian band shape with a width of 40 cm^{-1}.[5] At the same time, the absorption of 0.85 W m^{-2} by

[4]Most of this absorption, however, unlike the CAVIAR extra absorption relative to MTCKD, is localized in the near wings of the water vapour bands rather than in the windows [37].

[5]The calculations [30] provide the strength at the band centre, but, to apply them to atmospheric calculations, assumptions have to be made regarding the shape and width of these bands.

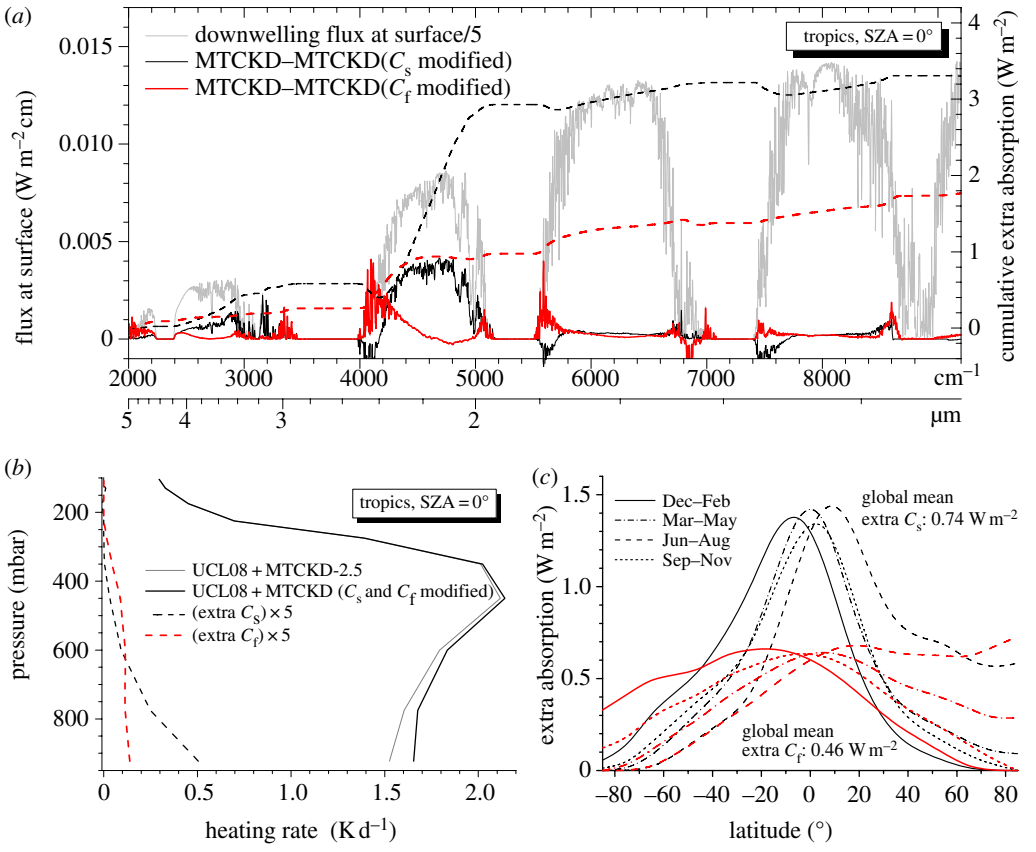

Figure 7. (*a*) The calculated spectrum of downwelling clear-sky solar irradiance at the surface (reduced by a factor of 5) and the extra absorption caused by modification of the self-continuum (C_s) according to Ptashnik *et al.* [16] and the foreign continuum (C_f) (this work) in the windows when compared with the MTCKD-2.5 model. The dashed lines show the respective cumulative extra absorptions (right axis). (*b*) The calculated clear-sky atmospheric heating rates and extra heating (increased by a factor of 5) due to modification of the self- and foreign continuum relative to MTCKD-2.5. The calculations in (*a*,*b*) are for a tropical atmosphere, overhead sun and a column water vapour amount of 4.7 g cm^{-2}. (*c*) The latitudinal dependence of the extra absorption owing to the self- [16] and new foreign continuum (this work), calculated for four seasons, using latitudinally and seasonally varying profiles of temperature and humidity taken from Christidis *et al.* [34]. (Online version in colour.)

$H_2O{-}H_2O$ complexes estimated in Kjaergaard *et al.* [30] for the same conditions is much less than our experimentally updated values for the self-continuum absorption of 6.5 W m^{-2}. The most part of this disagreement, however, can be clearly attributed to the fact that the dimerization equilibrium constant $K_{eq}(H_2O{-}H_2O) = 0.0123\,\text{atm}^{-1}$ used in Kjaergaard *et al.* [30] to account for the dimer amount at the surface was three to four times smaller than the average value 0.04–0.05 atm^{-1}, which can be deduced from the totality of the most recent theoretical and experimental works [13,38]. The last column of table 4 applies a factor of 4 to the $H_2O{-}H_2O$ result [30] to account for this modification. It also applies an extra factor of 1.5 to both the $H_2O{-}H_2O$ and $H_2O{-}(N_2$ and

Table 4. Estimated contribution ($W\,m^{-2}$) to absorption of near-infrared solar radiation for a tropical atmosphere (water vapour column amount of $4.7\,g\,cm^{-2}$) and overhead sun. Columns 2 and 3: due to, respectively, MTCKD-2.5 [9,10] and CAVIAR self- [16] and foreign (this work) continuum, compared with a 'no continuum' case. Column 4: due to $H_2O{-}N_2$ and $H_2O{-}O_2$ complexes, as estimated in Kjaergaard *et al.* [30] using a Lorentzian band width of $40\,cm^{-1}$ and equilibrium constants at the surface: $K_p(H_2O{-}H_2O) = 1.23 \times 10^{-2}$; $K_p(H_2O{-}N_2) = 7.53 \times 10^{-4}$; $K_p(H_2O{-}O_2) = 4.3 \times 10^{-3}$. Last column: same as column 4, but a modification is applied so that a value of $K_p(H_2O{-}H_2O) = 5.0 \times 10^{-2}$ is used and a band width of $60\,cm^{-1}$ is assumed, in place of the values used in Kjaergaard *et al.* [30] (see the text).

component	MTCKD-2.5	CAVIAR continuum	complexes [30]	complexes [30], modified
$H_2O{-}H_2O$	3.2	6.5	0.85	5.1
$H_2O{-}(N_2$ and $O_2)$	1.85	3.7	2.3	3.45

O_2) results [30] to account for a larger band width of $60\,cm^{-1}$ (compared with $40\,cm^{-1}$ in Kjaergaard *et al.* [30]). The latter was found to be a reasonably good first approximation for water dimer Lorentzian sub-bands to describe the self-continuum spectral features within near-infrared bands [11–14], and even the strength of the continuum in the windows [14,16] at close to standard temperatures. As a result, there is quite good agreement between the radiative impact of the experimental self- and foreign CAVIAR continuum (column 3) and the modified results of Kjaergaard *et al.* [30] for H_2O complexes (last column in table 4) made using their assumption of Lorentzian wings.

In spite of this agreement, the situation within the window regions may not be that straightforward. The far wings of bands of water complexes may deviate strongly from the Lorentzian shape. The weak local out-of-band combinational + librational sub-bands of these complexes may also make some contribution within the windows. Finally, at different temperatures, there may be different dominant contributors to the out-of-band foreign continuum: from true bound and quasi-bound complexes to the free-pair collisions (which also include far wings of monomer lines) [14]. All these considerations may complicate the situation and make it impossible to apply a general (for example, across a broad temperature range) description of the out-of-band continuum using just a simple Lorentzian band-width approach.

For the same conditions (tropical atmosphere, overhead sun), figure 7*b* shows the calculated atmospheric heating rate owing to the extra absorption using the CAVIAR self- and foreign continuum in the 2000–10 000 cm^{-1} spectral region when compared with the MTCKD-2.5. The contribution of the CAVIAR foreign continuum is more constant with height than the self-continuum, as it is proportional to vapour pressure rather than to the square of the vapour pressure. Finally, figure 7*c* presents the latitudinal dependence of the extra absorption due to the CAVIAR self- [16] and foreign continuum, calculated for four seasons, using latitudinally and seasonally varying profiles of temperature and humidity taken from Christidis *et al.* [34]. The global-mean value of the foreign-continuum extra absorption, relative to MTCKD-2.5, is $0.46\,W\,m^{-2}$, which is approximately 0.6 per cent of the total clear-sky absorption. For comparison, the additional

self-continuum absorption [16] is 0.74 W m^{-2}. The additional foreign-continuum absorption is less strongly peaked in the tropics than is the case for the self-continuum absorption [16], again because the latter's absorption scales with the square of the vapour pressure.

7. Conclusions

Based on new high spectral resolution laboratory measurements, we retrieved the water vapour foreign continuum within four near-infrared transmission windows for temperatures from 350 to 430 K. In the 4 µm window, these measurements support the conclusions of recent experiments by Baranov [18], which indicate that the foreign continuum in existing models is significantly underestimated in this window by typically one to two orders of magnitude. Moreover, our results extend this conclusion to the 2.1, 1.6 and (qualitatively) 1.25 µm windows, where we present what we believe to be the first retrieval of the foreign continuum. In all windows, the temperature dependence of the cross section of the derived foreign continuum is weak within the investigated range of temperatures.

Our results have implications for the understanding of the fundamental causes of the foreign continuum. The strength of the detected absorption is not consistent with the current understanding of the contribution of the far wings of water monomer lines. In most of the 4 µm windows, the water vapour foreign continuum can be reasonably well explained by N_2-H_2O BA arising from a collision-induced N_2 fundamental band [25,27]. In the 2.1 and 1.6 µm windows, overtones of the N_2 CIA band and interaction-modified transitions in the H_2O molecule, including those due to H_2O-N_2 and H_2O-O_2 complexes, might be the dominant cause of the H_2O foreign continuum, but further theoretical work is needed to establish whether or not this is the case. Further experimental work is necessary to establish the strength of the foreign continuum under near-atmospheric conditions and to clarify whether there is indeed weak temperature dependence, as might be expected from theoretical considerations. Additionally, experiments in which the H_2O-N_2 and H_2O-O_2 components (as well as other components) are derived separately would be valuable.

The new results show that the water vapour foreign continuum may make a substantial (up to 30–50%) contribution to the total atmospheric continuum in some spectral regions within the investigated windows. The estimated increase in the calculated clear-sky atmospheric absorption of solar radiation due to the new foreign continuum may reach approximately 0.6 per cent for the global mean and 1.5–2% in the tropics relative to the MTCKD-2.5 model.

This research was supported by the NERC-EPSRC consortium CAVIAR. NERC supported the use of the RAL Molecular Spectroscopy Facility. I.V.P. also acknowledges partial support from the Russian National contract 02.740.11.5198, RFBR grant 10-05-93105 in the frame of GDRI 'SAMIA' and RFBR grant 10-05-92603-KO. We are grateful to the reviewers for their detailed comments.

References

1 Kiehl, J. T. & Trenberth, K. E. 1997 Earth's annual global mean energy budget. *Bull. Am. Meteor. Soc.* **78**, 197–208. (doi:10.1175/1520-0477(1997)078<0197:EAGMEB>2.0.CO;2)

2 Clough, S. A., Iacono, M. J. & Moncet, J.-L. 1992 Line-by-line calculations of atmospheric fluxes and cooling rates: application to water vapour. *J. Geophys. Res.* **97**, 15 761–15 785. (doi:10.1029/92JD01419)

3 Kilsby, C. G., Edwards, D. P., Saunders, R. W. & Foot, J. S. 1992 Water-vapour continuum absorption in the tropics: aircraft measurements and model comparisons. *Q. J. R. Meteorol. Soc.* **118**, 715–748. (doi:10.1002/qj.49711850606)

4 Elsasser, W. M. 1938 Note on atmospheric absorption caused by the rotational water band. *Phys. Rev.* **53**, 768. (doi:10.1103/PhysRev.53.768)

5 Bignell, K. J. 1970 Water-vapour infra-red continuum. *Q. J. R. Meteorol. Soc.* **96**, 390–403. (doi:10.1002/qj.49709640904)

6 Nesmelova, L. I., Rodimova, O. B. & Tvorogov, S. D. 1986 [*Spectral line shape and intermolecular interaction*]. Novosibirsk, Russia: Nauka. [In Russian.]

7 Clough, S. A., Kneizys, F. X. & Davies, R. W. 1989 Line shape and the water vapour continuum. *Atmos. Res.* **23**, 229–241. (doi:10.1016/0169-8095(89)90020-3)

8 Tipping, R. H. & Ma, Q. 1995 Theory of the water vapour continuum and validations. *Atmos. Res.* **36**, 69–94. (doi:10.1016/0169-8095(94)00028-C)

9 Clough, S. A., Shephard, M. W., Mlawer, E., Delamere, J. S., Iacono, M., Cady-Pereira, K., Boukabara, S. & Brown, P. D. 2005 Atmospheric radiative transfer modeling: a summary of the AER codes. *J. Quant. Spectrosc. Radiat. Transf.* **91**, 233–244. (doi:10.1016/j.jqsrt.2004.05.058).

10 Mlawer, E. J., Payne, V. H., Moncet, J.-L., Delamere, J. S., Alvarado, M. J. & Tobin, D. C. 2012 Development and recent evaluation of the MT_CKD model of continuum absorption. *Phil. Trans. R. Soc. A* **370**, 2520–2556. (doi:10.1098/rsta.2011.0295)

11 Ptashnik, I. V., Smith, K. M., Shine, K. P. & Newnham, D. A. 2004 Laboratory measurements of water vapour continuum absorption in spectral region 5000–5600 cm^{-1}: evidence for water dimers. *Q. J. R. Meteorol. Soc.* **130**, 2391–2408. (doi:10.1256/qj.03.178).

12 Paynter, D. J., Ptashnik, I. V., Shine, K. P., Smith, K. M., McPheat, R. & Williams, R. G. 2009 Laboratory measurements of the water vapour continuum in the 1200–8000 cm^{-1} region between 293 K and 351 K. *J. Geophys. Res.* **114**, D21301. (doi:10.1029/2008JD011355).

13 Ptashnik, I. V. 2008 Evidence for the contribution of water dimers to the near-IR water vapour self-continuum. *J. Quant. Spectrosc. Radiat. Transf.* **109**, 831–852. (doi:10.1016/j.jqsrt.2007.09.004).

14 Ptashnik, I. V., Shine, K. P. & Vigasin, A. A. 2011 Water vapour self-continuum and water dimers. 1. Analysis of recent work. *J. Quant. Spectrosc. Radiat. Transf.* **112**, 1286–1303. (doi:10.1016/j.jqsrt.2011.01.012).

15 Baranov, Y. I. & Lafferty, W. J. 2011 The water-vapour continuum and selective absorption in the 3 to 5 μm spectral region at temperatures from 311 to 363 K. *J. Quant. Spectrosc. Radiat. Transf.* **112**, 1304–1313. (doi:10.1016/j.jqsrt.2011.01.024).

16 Ptashnik, I. V., McPheat, R. A., Shine, K. P., Smith, K. M. & Williams, R. G. 2011 Water vapor self-continuum absorption in near-infrared windows derived from laboratory measurements. *J. Geophys. Res.* **116**, D16305 (doi:10.1029/2011JD015603).

17 Burch, D. E. 1985 Absorption by H_2O in narrow windows between 3000 and 4200 cm^{-1}. US Air Force Geophysics Laboratory report AFGL-TR-85–0036. Hanscom Air Force Base, MA, USA.

18 Baranov, Y. I. 2011 The continuum absorption in $H_2O + N_2$ mixtures in the 2000–3250 cm^{-1} spectral region at temperatures from 326 to 363K. *J. Quant. Spectrosc. Radiat. Transf.* **112**, 2281–2286. (doi:10.1016/j.jqsrt.2011.06.005)

19 White, J. U. 1942 Long optical paths of large aperture. *J. Opt. Soc. Am.* **32**, 285–288. (doi:10.1364/JOSA.32.000285)

20 Shillings, A. J. L., Ball, S. M., Barber, M. J., Tennyson, J. & Jones, R. L. 2011 An upper limit for water dimer absorption in the 750 nm spectral region and a revised water line list. *Atmos. Chem. Phys.* **11**, 4273–4287. (doi:10.5194/acp-11-4273-2011).

21 Mitsel, A. A., Ptashnik, I. V., Firsov, K. M. & Fomin, B. A. 1995 Efficient technique for line-by-line calculating the transmittance of the absorbing atmosphere. *Atmos. Oceanic Opt.* **8**, 847–850.

22 Rothman, L. S. *et al.* 2009 The HITRAN 2008 molecular spectroscopic database. *J. Quant. Spectrosc. Radiat. Transf.* **110**, 533–572. (doi:10.1016/j.jqsrt.2009.02.013).

23 Brown, A. & Tipping, R. H. 2003 Collision-induced absorption in dipolar molecule-homonuclear diatomic pairs. In *Proc. NATO Advanced Research Workshop. Weakly interacting molecular pairs: unconventional absorbers of radiation in the atmosphere* (eds C. Camy-Peyret & A. A. Vigasin), pp. 93–99. Dordrecht, The Netherlands: Kluwer Academic Publishers.

24 Hartmann, J. M., Perrin, M. Y., Ma, Q. & Tipping, R. H. 1993 The infrared continuum of pure water vapour: calculations and high-temperature measurements. *J. Quant. Spectrosc. Radiat. Transf.* **49**, 675–691. (doi:10.1016/0022-4073(93)90010-F)

25 Bykov, A. D., Lavrentieva, N. N., Sinitsa, L. N. & Solodov, A. M. 2001 Influence of the intramolecular resonances on the interference of water vapour spectral lines. *Atmos. Oceanic. Opt.* **14**, 774–780.

26 Frommhold, L. 2006 *Collision-induced absorption in gases*. Cambridge, UK: Cambridge University Press.

27 Baranov, Yu. I., Buryak, I. A., Lokshtanov, S. E., Lukyanchenko, V. A. & Vigasin, A. A. 2012 $H_2O{-}N_2$ collision-induced absorption band intensity in the region of the N_2 fundamental: *ab initio* investigation of its temperature dependence and comparison with laboratory data. *Phil. Trans. R. Soc. A* **370**, 2691–2709. (doi:10.1098/rsta.2011.0189)

28 Vigasin, A. A. 2000 Water vapour continuous absorption in various mixtures: possible role of weakly bound complexes. *J. Quant. Spectrosc. Radiat. Transf.* **64**, 25–40. (doi:10.1016/S0022-4073(98)00142-3)

29 Vigasin, A. A. 2003 Bimolecular absorption in atmospheric gases. In *Proc. NATO Advanced Research Workshop. Weakly interacting molecular pairs: unconventional absorbers of radiation in the atmosphere* (eds C. Camy-Peyret & A. A. Vigasin), pp. 23–47. Dordrecht, The Netherlands: Kluwer Academic Publishers.

30 Kjaergaard, H. G., Robinson, T. W., Howard, D. L., Daniel, J. S., Headrick, J. E. & Vaida, V. 2003 Complexes of importance to the absorption of solar radiation. *J. Phys. Chem. A* **107**, 10 680–10 686. (doi:10.1021/jp035098t).

31 Vigasin, A. A. 1991 Bound, metastable and free states of bimolecular complexes. *Infrared Phys.* **32**, 461–470. (doi:10.1016/0020-0891(91)90135-3)

32 Lokshtanov, S. E., Ivanov, S. V. & Vigasin, A. A. 2005 Statistical physics partitioning and classical trajectory analysis of the phase space in CO_2–Ar weakly interacting pairs. *J. Mol. Struct.* **742**, 31–36. (doi:10.1016/j.molstruc.2004.12.055)

33 Cormier, J. G., Hodges, J. T. & Drummond, J. R. 2005 Infrared water continuum absorption at atmospheric temperatures. *J. Chem. Phys.* **122**, 114309. (doi:10.1063/1.1862623).

34 Christidis, N., Hurley, M. D., Pinnock, S., Shine, K. P. & Wallington, T. J. 1997 Further calculations of the radiative forcing of CFC-11 and possible fluorocarbon replacements to the CFCs. *J. Geophys. Res.* **102**, 19 597–19 609. (doi:10.1029/97JD01137)

35 Stamnes, K., Tsay, S. C., Wiscombe, W. & Jayaweera, K. 1988 A numerically stable algorithm for discrete-ordinate-method transfer in multiple scattering and emitting layered media. *Appl. Opt.* **27**, 2502–2509. (doi:10.1364/AO.27.002502)

36 Fontenla, J. O., White, R., Fox, P. A., Avertt, E. H. & Kurucz, R. L. 1999 Calculation of solar irradiances. I. Synthesis of the solar spectrum. *Astrophys. J.* **518**, 480–518. (doi:10.1086/307258)

37 Ptashnik, I. V. & Shine, K. P. 2003 Calculation of solar radiative fluxes in the atmosphere: the effect of updates in spectroscopic data. *Atmos. Oceanic Opt.* **16**, 251–255.

38 Scribano, Y., Goldman, N., Saykally, R. J. & Leforestier, C. 2006 Water dimers in the atmosphere III: equilibrium constant from a flexible potential. *J. Phys. Chem. A* **110**, 5411–5419. (doi:10.1021/jp056759k).